Springer Proceedings in Earth and Environmental Sciences

Gevorg Kocharyan
Andrey Lyakhov *Editors*

Trigger Effects in Geosystems

The 5th International Conference, Sadovsky Institute of Geospheres Dynamics of Russian Academy of Sciences

EXTRAS ONLINE

Springer

Springer Proceedings in Earth and Environmental Sciences

The series Springer Proceedings in Earth and Environmental Sciences publishes proceedings from scholarly meetings and workshops on all topics related to Environmental and Earth Sciences and related sciences. This series constitutes a comprehensive up-to-date source of reference on a field or subfield of relevance in Earth and Environmental Sciences. In addition to an overall evaluation of the interest, scientific quality, and timeliness of each proposal at the hands of the publisher, individual contributions are all refereed to the high quality standards of leading journals in the field. Thus, this series provides the research community with well-edited, authoritative reports on developments in the most exciting areas of environmental sciences, earth sciences and related fields.

More information about this series at http://www.springer.com/series/16067

Gevorg Kocharyan · Andrey Lyakhov
Editors

Trigger Effects in Geosystems

The 5th International Conference, Sadovsky Institute of Geospheres Dynamics of Russian Academy of Sciences

Springer

Editors
Gevorg Kocharyan
Sadovsky Institute of Geospheres
Dynamics RAS
Moscow, Russia

Andrey Lyakhov
Sadovsky Institute of Geospheres
Dynamics RAS
Moscow, Russia

ISSN 2524-342X ISSN 2524-3438 (electronic)
Springer Proceedings in Earth and Environmental Sciences
ISBN 978-3-030-31969-4 ISBN 978-3-030-31970-0 (eBook)
https://doi.org/10.1007/978-3-030-31970-0

This Springer imprint is published by the registered company Springer Nature Switzerland AG
The registered company address is: Gewerbestrasse 11, 6330 Cham, Switzerland

Introduction

The Fifth International Conference "Trigger Effects in Geosystems" was organized by the Sadovsky Institute of Geospheres Dynamics of Russian Academy of Sciences, and was held on June 4–7, 2019 in Moscow, Russia.

The understanding of how the processes of nucleating instabilities in geosystems are triggered by external effects is extremely important in terms of elaborating new approaches to the problem of prediction and prevention of natural and anthropogenic catastrophes. Investigating trigger processes is very attractive, because these phenomena are one of the rare possibilities to detect the cause-and-effect relations in studying the dynamics of large-scale natural objects. Activities in this direction can suggest new ways in developing the strategy of forecasting and preventing geocatastrophes or, at least, lowering the damage. More than 250 scientific specialists, students, and postgraduates from institutes of the Russian Academy of Sciences, universities, and other Russian and foreign organizations took part in the Conference.

The Conference considered the following scientific problems:

- Exogenous triggering of deformation processes in the Earth's crust. Monitoring and forecasting trigger effects. Trigger effects in geology.
- Structure and properties of fault zones. Different sliding regimes on faults. Links to seismicity.
- Safety of mining operations. Deformation processes in mining activities. Fault-slip rock bursts. Mining seismicity. Stability of engineering constructions.
- Seismicity in developing hydrocarbon deposits and hydrocarbon recovery. Geomechanics and fluid dynamics of rock massifs.
- Geophysical fields. Their variations and interactions.
- Active disturbances of ionosphere and magnetosphere of the Earth. Experimental results, numerical and theoretical models.
- The global current circuit, electrical and optical processes in the atmosphere, in equilibrium plasma chemistry of atmospheric phenomena.
- Experimental data and theoretical models of the response of ionosphere to catastrophic natural events (fall of cosmic objects, earthquakes, tsunamis, volcanic eruptions, powerful cyclones).

Conference proceedings are published in two books. The reports presented in English are published in this book. For convenience, all the articles are structured into parts. The first part deals with trigger effects in the solid Earth. The second part is devoted to dynamic processes that emerge in the course of mining activities. The final part combines articles that consider dynamic effects in the upper geospheres.

The organizing committee thanks the Russian Foundation for Basic Research and the Ministry of Science and Higher Education for financial support.

Prof. Gevorg Kocharyan
Dr. Andrey Lyakhov

Contents

Trigger Effects in Solid Earth

Modeling Modern Geotectonic Processes of the Siberian Platform and Its Margins 3
Ayan Akhmetov, Pavel Makarov, Igor Smolin and Alexey Peryshkin

Formalized Forecast of the Gutenberg-Richter Law Parameters by Geodynamic and Seismotectonic Data 13
Eugeny Bugaev and Svetlana Kishkina

Statistical Regularities of a Main Crack Formation in Rocks. Acoustic Emission and X-Ray Computed Microtomography 23
Ekaterina Damaskinskaya, Vladimir Hilarov, Ivan Panteleev, Dmitry Korost and Dmitry Frolov

Numerical Modelling of Formation of Chuya-Kuray Fault Zone, Gorni Altai 33
Mikhail Eremin and Yurii Stefanov

Indicators of Changes in the Stress-Strain State of the Geoenvironment in the Preparation and Realization of Strong Tectonic Earthquakes According to Long-Term Measurements with Underground Electric Antennas 43
Valery Gavrilov, Alexey Deshcherevskii, Yuliya Buss, Yuliya Morozova, Ivan Panteleev, Yuriy Vlasov, Oleg Fedoristov and Vladimir Denisenko

Earth's Natural Pulsed Electromagnetic Field (ENPEMF) Temporal Variation Anomalies as Earthquake Precursors 53
Vasiliy Gordeev, Sergey Malyshkov, Vitaly Polivach and Sergey Shtalin

Formalized Lineament Analysis as a Basis for Seismic Monitoring of Platform Areas 61
Galina Ivanchenko and Svetlana Kishkina

Migration of Earth Surface Deformation as a Large Earthquake Trigger 71
Vladimir Kaftan and Andrey Melnikov

Development of Geomechanical Model of the South Segment of Central Sakhalin Fault Zone 79
Pavel Kamenev, Leonid Bogomolov and Andrey Zabolotin

Mathematical Modeling of Dynamic Processes in Seismic Activity Zones 87
Alexandr Kim, Yuriy Shpadi and Yuriy Litvinov

Effect of Multiple Weak Impacts on Evolution of Stresses and Strains in Geo-materials 95
Vladimir Kosykh

Modeling Accumulation and Release of Energy in a Geo-medium Under the Influence of Tidal Forces 105
Sergey Lavrikov and Alexander Revuzhenko

Optimal Methods and Parameters of Electromagnetic Monitoring in Seismically Active Areas 115
Nina Nevedrova and Aleksandr Shalaginov

Fault Block Structure of Gorny Altai Intermountain Areas According to Geoelectrical Data 125
Nina Nevedrova, Aydisa Sanchaa, Ilya Shaparenko and Sergey Babushkin

Geoelectrical Models of Fault Zones in the Gorny Altai Region 135
Nina Nevedrova, Sergey Babushkin, Aydisa Sanchaa, Ilya Shaparenko and Alexander Shalaginov

Rotation Factor: Dynamics and Interaction of the Earth's Core and Mantle 145
Vladimir Ovtchinnikov and Dmitry Krasnoshchekov

Fault Complexity and Interaction: Evidence of Static Earthquake Triggering 153
Eleftheria Papadimitriou and Vasileios Karakostas

On the Results of Studying Deep Paleo Seismic Dislocations (at the Example of the Marginal Suture of the Siberian Craton) 163
Valery Ruzhich, Alexey Ostapchuk and Dmitry Pavlov

Effect of Changing Basal Friction on the Formation of Thrust 169
Antonina Tataurova, Yurii Stefanov and Vladimir Suvorov

Calculation of Filtration Properties of the Antey Uranium Deposit Rock Massif at the Deformation Phases: Microstructural Approach 179
Stepan Ustinov, Vladislav Petrov, Valery Poluektov and Vasily Minaev

Trigger Effect of a Heat Flow on Distribution of Critical Level of Deformations in Focal Zones 187
Andrey Vilayev

Properties and Type of Latitudinal Dependence of Statistical Distribution of Geomagnetic Field Variations 197
Andrei Vorobev and Gulnara Vorobeva

Destruction of Artificial Sandstone Samples in a State Close to Unstable with Electrical Pulses 207
Vladimir Zeigarnik, Vadim Kliuchkin and Vladimir Okunev

Fluidodynamic Processes and Seismicity

Apparent Permeability Loss Over Time in Long-Term Measurements Using the Steady-State Method 221
Nikolay Baryshnikov, Evgeniy Zenchenko and Sergey Turuntaev

Experimental Study of the Effect of Plastic Rock Properties on Hydraulic Fracturing 229
Igor Faskheev and Maria Trimonova

Features of Fluid-Dynamic Processes in a Seismically Active Region (Case Study of Kamchatka Peninsula, Russia) 237
Galina Kopylova and Svetlana Boldina

Analysis of Crack Formation in Model Specimens During Hydraulic Fracturing in Holes 247
Arkady Leontiev and Ekaterina Rubtsova

Determination of Filtration Properties and Mass Transfer Coefficient for Fractured Porous Media by Laboratory Test Data 257
Larisa Nazarova and Leonid Nazarov

Hydraulic Fracturing Pressure Curves as a Way for Determining Reservoir Parameters 269
Helen Novikova and Mariia Trimonova

Modeling of Fault Deformation Driven by Fluid Injection 279
Vasily Riga and Sergey Turuntaev

Measurement of Gas-Dynamic Parameters of Superheated Gas Flow in Slit, Applicable to the Bazhenov Formation 289
Aliya Tairova and Georgy Belyakov

Structural Transformations of the Nanoconfined Water at High Pressures: A Potential Factor for Dynamic Rupture in the Subduction Zones 297
Alexey Tsukanov, Evgeny Shilko and Sergey Psakhie

Dynamic Processes in Mining

Inrush of Ay River Water into Kurgazakskaya Mine Workings as Trigger of Tectonic Rock Burst 309
Andrian Batugin

Triggering Tectonic Earthquakes by Mining 319
Gevorg Kocharyan, Alexander Budkov and Svetlana Kishkina

Dynamics of Rock Mass Seismicity During Mining Near the Saamsky Fault in the Kirovsky Mine, Apatit JSC 329
Anatoly Kozyrev, Svetlana Zhukova and Olga Zhuravleva

An Integrated Approach for Prediction of Hazardous Dynamic Events (Case Study of Retrospective Data in the Area of a Tectonic Rockburst in the Rasvumchorr Mine on January 9, 2018) 339
Anatoly Kozyrev, Olga Zhuravleva and Inna Semenova

Regularities of Increase and Decrease of the Triggered Seismicity in the Rock Mass During the Lovozero Rare-Metal Deposit Development 349
Aleksandr Lovchikov

A Study of the Trigger Effect in a Rock Burst-Hazard Rock Massif by Laser Interferometry 357
Vladimir Lugovoy, Grigoriy Dolgikh, Denis Tsoy, Andrey Gladyr and Maksim Rasskazov

Stress-Strain State Monitoring of a Man-Induced Landslide Based on the Lithospheric Component Parameters of the Earth's Pulsed Electromagnetic Field 367
Sergey Malyshkov, Vasiliy Gordeev, Vitaliy Polivach and Sergey Shtalin

The Analysis of Conditions of Geodynamic Process Activation and Manifestation of Technogenic Seismicity on Underground Mines of the Far East Region 379
Igor Rasskazov, Vladimir Lugovoy, Denis Tsoy and Alexander Sidlyar

Determination of Critical Deformation and Destruction Parameters of the Zhelezny Open Pit Rock Mass (JSC Kovdorsky GOK) Based on IBIS FM Ground Radar Data 387
Ivan Rozanov and Aleksander Zavialov

Causal Factors of Mudflows (a Study of the Tyrnyauz Tungsten-Molybdenum Plant in Tyrnyauz City Kabardino-Balkarian Republic) 395
Zalim Terekulov

On Deformation Stability of Rock Massif 407
Vitaly Trofimov

About Interaction of Blasting and Geomechanical Processes in Mining 417
Sergey Viktorov, Vladimir Zakalinsky, Ivan Shipovskii and Rafael Mingazov

Methane Generation During Coal Failure 427
Valery Zakharov and Olga Malinnikova

About Order of Comprehensive Solving the Seismic and Pre-splitting Issues for Drill-and-Blastin Open-Pits 437
Sergey Zharikov and Vyacheslav Kutuev

Dynamic Effects in Upper Geospheres

Analysis of the Probability Fields of Ionospheric Parameters Used for the Probabilistic Plasma-Chemical Modeling of the Lower Ionosphere 449
Bekker Susanna

A Mathematical Model of the Ionospheric Electric Field Which Closes the Global Electric Circuit 455
Valery Denisenko, Michael Rycroft and R. Giles Harrison

Experimental Study of Mid-latitude Ionosphere Disturbances Caused by Auroral Phenomena and Heating Experiments 465
Boris Gavrilov, Julius Zetzer, Yuriy Poklad, Iliya Ryakhovskiy, Andrey Lyakhov, Vladimir Rybakov, Dmitriy Egorov and Vladimir Ermak

Scaling Relations for Shock Wave Effects from the Impacts of Cosmic Objects with Diameters from a Few Meters to 3 Km 475
Dmitry Glazachev, Elena Podobnaya, Olga Popova, Vladimir Svetsov, Valery Shuvalov and Natalia Artemieva

Effects of the Impact of Jet Engines of Progress Spaceships on the Ionosphere According to GPS Receivers of the Japanese Network GEONET 487
Artem Ishin, Sergey Voeykov and Vitaly Khakhinov

Acoustic Fluidization During Impact Crater's Formation 497
Boris Ivanov

Dust Particle Dynamics in Convective Vortices Near the Surface of the Earth: Comparison with Mars 507
Yulia Izvekova, Sergey Popel and Oleg Izvekov

The Lower Atmosphere Response to Seismic Events Using Satellite Data 515
Valentine Kashkin, Roman Odintsov, Tatyana Rubleva, Alexey Romanov and Konstantin Simonov

Chicxulub Impact as a Trigger of One of Deccan Volcanism Phases: Threshold of Seismic Energy Density 523
Valery Khazins and Valery Shuvalov

Studies of the Disturbances of the Geomagnetic Field in the 0.001–0.03 Hz Range Under Influence on the Ionosphere by Powerful Radio Emission of the SURA Facility 531
D. S. Kotik, A. V. Ryabov, V. I. Ivanov, V. P. Esin and D. V. Myazdrikov

Simulation of Aluminum Jet Expansion in Active Geophysical Experiments Taking into Account Deviation of Ionization State from Thermodynamic Equilibrium 537
Marina Kuzmicheva

VLF Emission Excited by Electric Generator Mounted on Satellite INTERCOSMOS-24 547
Yuriy Mikhailov

The Influence of the Magnetic Field Inclination on the Quasistationary Electric Field Penetration from the Ground to the Ionosphere 559
Semen Nesterov, Valery Denisenko, Mohammed Yahia Boudjada and Helmut Lammer

Scaling Relations for Radiation Effects Due to Impacts of Large Cosmic Objects 569
Elena Podobnaya, Dmitry Glazachev, Olga Popova, Vladimir Svetsov and Valery Shuvalov

Trigger Excitation of IPDP ULF Waves (Maltseva–Vinogradova Effect) 579
Alexander Potapov, Boris Dovbnya, Boris Klain and Anatol Guglielmi

Trigger Effect of an Asteroidal or Cometary Impact at the Permian–Triassic Boundary 589
Vladimir Svetsov and Valery Shuvalov

Seismo-acoustic Effects of the Lipetsk Bolide 21.06.2018 597
Alexander Varypaev, Sergey Volosov, Natalia Konstantinovskaya, Margarita Nesterkina, Vladimir Kharlamov and Yuriy Rybnov

Nightside Magnetic Impulsive Events: Statistics and Possible Mechanisms 607
Andrei Vorobev, Vyacheslav Pilipenko and Mark Engebretson

Part I
Trigger Effects in Solid Earth

Modeling Modern Geotectonic Processes of the Siberian Platform and Its Margins

Ayan Akhmetov, Pavel Makarov, Igor Smolin and Alexey Peryshkin

Abstract

This article presents the numerical modeling of modern tectonic flows in the Siberian Craton. It is based on global geotectonic processes in the Asian continent as well as its geological structure. The margins of Siberian Craton are unstable geological structures where local active geotectonic processes such as collision, shear stretching and metamorphisms are observed. We selected the region of the Yenisei Ridge because of its geological and geophysical specifics. The type of state of stress and strain in this area was estimated on the base of calculations of global tectonic flows in Central Asia. To get more details on the type of state of stress and strain in the Yenisei Ridge, calculations were carried out for the geological cross sections of Batolit 1982 and Shpat. The results show the presence of regions of localized inelastic deformation in the overstep region of the Yenisei shear zone. Also, in both sections, the bands of localized inelastic strain propagate to the surface of the mountain group exactly in the regions of the location of the large Siberian rivers of Yenisei and Velmo.

Keywords

Tectonic flow · Geological cross-section · State of stress and strain

A. Akhmetov (✉) · P. Makarov · I. Smolin
Tomsk State University, 634050 Tomsk, Russian Federation
e-mail: ayan.akhmetov93@gmail.com

A. Akhmetov · P. Makarov · I. Smolin · A. Peryshkin
Institute of Strength Physics and Materials Science SB RAS, 634055 Tomsk, Russian Federation

G. Kocharyan and A. Lyakhov (eds.), *Trigger Effects in Geosystems*,
Springer Proceedings in Earth and Environmental Sciences,
https://doi.org/10.1007/978-3-030-31970-0_1

1 Introduction

The fundamental geodynamic processes such as collision, subduction, and spreading are natural phenomena that often studied based on the concept of plate tectonics originating from the theory of continental drift [1]. Geophysical community has demonstrated great interest in investigating the tectonics of large Eurasian Plate and, particularly, its most dynamic parts in the Central and Southeastern Asia. The whole spectrum of tectonic processes can be observed in these regions. The Asian continent has seismically active intracontinental rifts, for instance, the Red River Rift (China) and the Baikal Rift Zone (Russian Federation). The Indian subduction resulting from collision of the Eurasian and Indian plates plays the main role in formation of tectonic flows in Central and Southeastern Asia [2]. These geotectonic processes lead to formation of the Tibetan Plateau and the Himalayan mountains (Asian mountain system). Collision of the American and Eurasian plates in the North-East also influenced the geodynamic situation of the Asian continent with formation of the Verkhoyansk Range and the Kolyma Mountains [3]. Geotectonic transformations in the Asian continent, from separation of Pangea into Gondwana and Laurasia to evolution of modern Asian mountain systems, have been in progress for about 300 million years. This overall mechanism of plate movement plays a minimal role in the research of regional tectonic flow. It is only accepted to evaluate initial and boundary conditions in the studied area.

Siberian Craton is one of the largest Archean-Proterozoic regions, which is a major part of Northern Eurasia. It is adjoined by geological objects with different structural properties [4, 5]. Particularly, the Yenisei Ridge is one of the interesting regions of the Siberian Craton with regard to research of the Asian continent. It is the major structural feature of the western margin between the Siberian Craton and the Central Asian fold belt and located along the Yenisei River. The geological composition of Yenisei Ridge comprises various terranes separated by faults [6, 7]. For this reason, interpreting its geotectonic structure and formation conditions is essentially used for regional and global geodynamic reconstruction of the Eurasian lithosphere.

Introduction and development of calculational technologies have made possible to simulate global and regional tectonic flows of the Earth's crust. Müller et al. developed a computer program that simulates the global geological phenomena using experimental and theoretical data from geophysics, geochemistry, and plate tectonics [8]. Actually, difficulties emerge when we research the regional tectonic flows. To investigate both global and regional tectonic flows in the Asian continent, a modern concept was suggested to analyze the plate tectonics. This concept can help to permit investigating the tectonic flow pattern and stress field as characteristics of the evolutionary process which is inhomogeneous in space and time [9, 10]. Nevertheless, specifics of upright movements and volumetric stress state in the Earth's crust can't be treated within this approach.

The purpose of this paper is to interpret the numerical investigations of regional geotectonic pattern in the Yenisei Ridge in terms of evolution of stress state and tectonic flows in Central Asia resulting from collision of the Eurasian Plate with Hindustan and Arabia in the South and with North America in the North-East. To achieve this goal, we have simulated the tectonic flow pattern in the Asian continent and the regional geotectonic state of the Siberian Craton. Finally, we have analyzed the collision state in the deep structure of the Yenisei Ridge using the data from Batolit-1982 and Shpat geological profiles.

2 Problem Statement

To investigate tectonic movement in Central and Southeast Asia (predominantly in the Siberian Craton), we made use of the Seminskii's scheme—a zone-block lithospheric structure of Eastern and Central Asia that is used here as a general structural model. The developed model contains also boundary blocks which aim to mimic real geodynamic effects from neighboring regions [11]. This model is shown in Fig. 1.

This structural model is two-dimensional and can provide only a two-dimensional picture of geotectonic movements, yet the boundary condition for analysis of deep structures of the Yenisei Ridge can be obtained from it.

The computer models of vertical cross-sections of the Earth's crust are evolved for analyzing the state of stress and strain using the Batolit-1982 and Shpat geological profiles obtained from deep seismic sounding method. Their orientation are shown in Fig. 2.

Two computer models of the Yenisei Ridge cross sections produced by using the corresponding geophysical data are shown in Fig. 3. The dimensions of the computer models for Batolit profile is 341 × 60 km and for Shpat profile is 288 × 60 km.

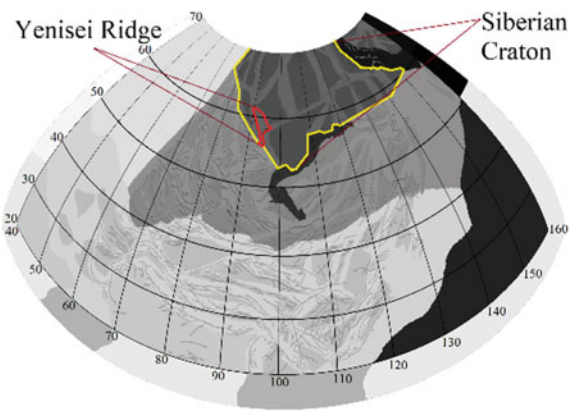

Fig. 1 Map of the numerical domain with the three groups of zone-block regions and boundary elastic blocks

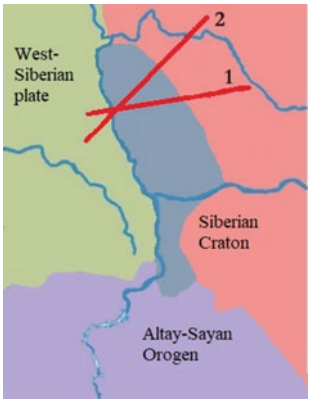

Fig. 2 Orientation of Batolit-1982 (1) and Shpat (2) geological profiles crossing the Yenisei Ridge

The lens colored in red in Fig. 3 is revealed up to depth of 10–12 km in these cross-sections. Other crust layers are also revealed by the difference in geological, physical and mechanical properties of the media. The profiles include different types of faults. They were simulated in the form of weakened zones at the edges of these faults. The P- and S-wave velocities determined during deep seismic sounding were used to estimate the elastic properties of each layer of the structural models.

The elements of the Earth's crust and upper mantle are poorly studied because of lack of direct experimental constraints on physical and mechanical properties of geomaterials that comprise the layers of the Earth's crust. For this reason, we adopted the fundamental models describing depth variation of geomaterial strength presented elsewhere [12–15]. Since, as known, pressure increases almost linearly with depth, it is possible to accept strength models for pressure sensitive materials. The popular Drucker–Prager strength criterion on the base of linear pressure dependence is introduced as

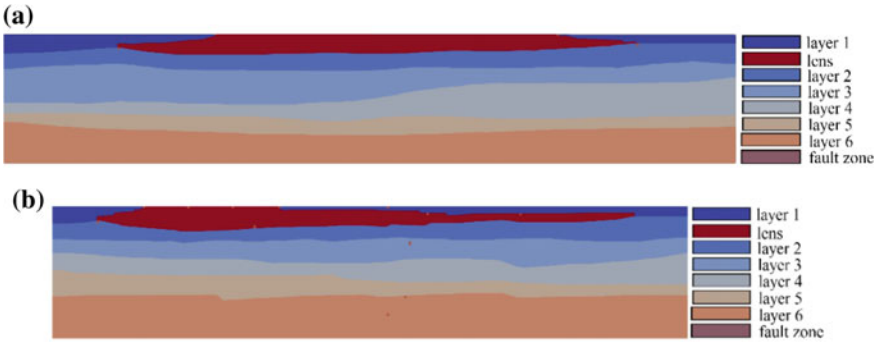

Fig. 3 Computer models of the Yenisei Ridge based on the Batolit-1982 (**a**) and Shpat (**b**) geological profiles

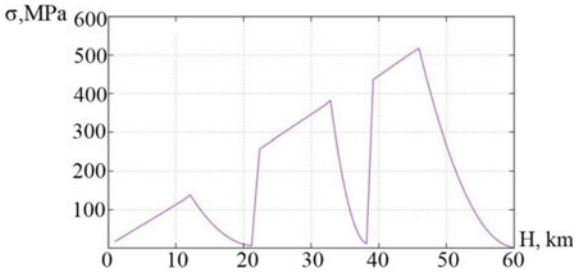

Fig. 4 Strength of the layers as a function of depth

$$\sigma = Y + \alpha \cdot P \tag{1}$$

where Y is the shear strength at zero pressure (cohesion), α is the friction coefficient, P is the pressure.

In fact, the depth dependence of strength is not monotonic, it has descending parts, and is often specified for continental plates in the form shown in Fig. 4 [12–16]. To meet such kind of relationship, the values of shear strength and friction coefficient are adopted as specific depth functions to get the strength-depth dependence with consideration for Eq. (1).

3 Mathematical Model

The fundamental equations of solid mechanics are included in the mathematical model that consists of the conservation laws and constitutive relations. The latter are formulated in rates. So, hypoelasticity equations characterize the elastic response of media. To describe the plastic response, the model of Drucker–Prager–Nikolaevskiy with non-associated flow rule is taken as a basis allowing for independent descriptions of dilatation and internal friction. In this case the equations read

$$f(\sigma_{ij}) = \frac{\alpha}{3} J_1 + J_2^{1/2} - Y = 0, \tag{2}$$

where $f(\sigma_{ij})$ is the yield surface and J_1, J_2 are the first and the second invariants of the stress tensor, Y is the current strength. In the case of non-associated flow rule, the plastic potential $g(\sigma_{ij})$ does not coincide with function of plasticity and according to Nikolaevskiy is written as follows [17]:

$$g(\sigma_{ij}) = J_2 + \frac{\Lambda}{3} J_1 \left(2Y - \frac{\alpha}{3} J_1\right) + const. \tag{3}$$

Here Λ is the dilatancy coefficient.

Components of rates of inelastic strains will be defined as follows:

$$\dot{\varepsilon}_{ij}^{p} = \dot{\lambda}\frac{\partial g(\sigma_{ij})}{\partial \sigma_{ij}} = \dot{\lambda}\left(s_{ij} + \frac{2}{3}\Lambda\left(Y - \frac{\alpha}{3}J_1\right)\delta_{ij}\right), \tag{4}$$

where $\dot{\lambda}$ is the plasticity multiplier in the theory of plasticity.

Peculiarities of the boundary value problem statement in the case of tectonic flow modeling are presented in [9, 10]. The numerical implementation is performed using the Wilkins finite-difference method [18].

4 Results and Discussion

Specific features of deformation and loading of the adopted geological areas that govern the stress state type in them are defined from the computation of tectonic flows in Central and Southeastern Asia. We made these calculations only for collision related processes between the Eurasian, Indian and Arabian plates. The results are illustrated in Fig. 5. They indicate that compression predominates in the Yenisei Ridge.

Calculations of tectonic flows also show that the compression direction in the Yenisei Ridge is perpendicular to the Yenisei regional shear zone [4], and the Batolit-1982 and Shpat geological cross-sections lie in the compression direction. Consequently, we can calculate strains and stresses in the cross sections along the Batolit-1982 and Shpat profiles under loading by compression lengthwise of the profiles. The distributions of plastic strains and horizontal stress obtained in the simulation are given in Figs. 6 and 7.

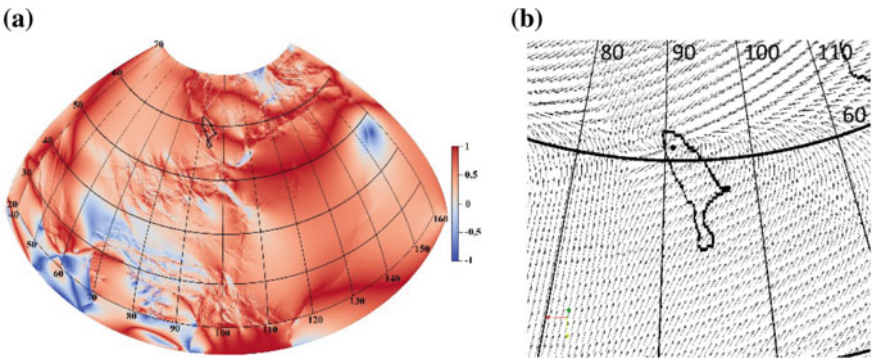

Fig. 5 Simulation results of tectonic flows in the Yenisei Ridge: **a** stress state type in Central and Southeastern Asia by the Lode parameter, **b** displacement fields determined in reference to the marked point

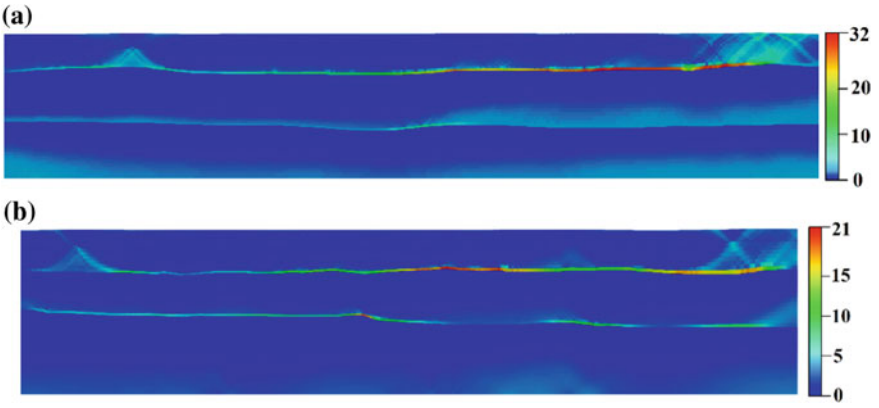

Fig. 6 Plastic strain (%) distributions in the Yenisei Ridge along the **a** Batolit-1982 and **b** Shpat profiles

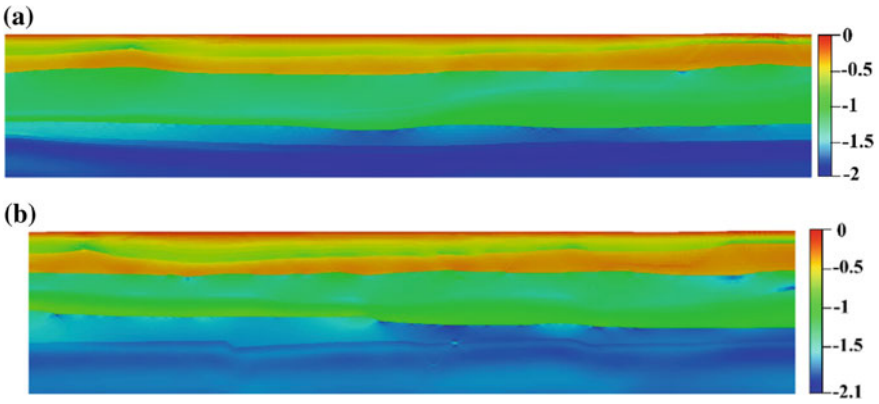

Fig. 7 Horizontal stress (GPa) distributions in the Yenisei Ridge along the **a** Batolit-1982 and **b** Shpat profiles

Analysis of the presented results yields the following. Fault zones are the places where plastic deformation and further evolution of localized strain originate from. The curvature of interfaces between the layers also affects localization of plastic strain. The internal friction and dilatancy that enter the Drucker–Prager–Nikolaevskiy plasticity law have an impact on the orientation of localized deformation bands. From the geological point of view, Fig. 6 evidences that in both cases deformation localizes in the Yenisei shear zone, which is located in the upper left part of the figures. In the right part of these figures, we can see another strain localization, which is consistent with the opposite side of the lens in the computer

models where the Velmo river is located. The stress field distribution is inhomogeneous and non-monotonously increase with depth due to the presence of physical and mechanical heterogeneities and curvature of interfaces between layers.

5 Conclusions

We solved the problem of computation of tectonic flows and the related stress state type in Central and Southeastern Asia caused by collision with the Indian and Arabian plates (in the South) and the North American Plate in the North-East. A special interest was to evaluate the stress state type in the Yenisei Ridge located to the South-West of the Siberian Craton. These calculations determined displacements of the Siberian Craton and allowed plotting the deformation pattern of Yenisei Ridge. The calculations also show that compression predominates in the Yenisei Ridge, the direction of compression being perpendicular to the Yenisei regional shear zone.

Calculations of depth distributions of stress and strain in the Yenisei Ridge along the Shpat and Batolit-1982 geological profiles show that the main factors determining nucleation sites of inelastic deformation and propagation of localized deformation bands are fault zones and curvature of interfaces between the layers. For both profiles, the plastic deformation distribution reveals deformation localization in the Yenisei shear zone and locations of the Velmo river. Variation in physical and mechanical properties and curvature of interfaces between layers result in heterogeneous and non-monotonous character of horizontal stress distribution.

Acknowledgments The work was carried out within the framework of the Fundamental Research Program of the State Academies of Sciences for 2013–2020, line of research III.23, and with the support of the Comprehensive Program of Fundamental Research of the Siberian Branch of Russian Academy of Sciences "Interdisciplinary Integration Studies" 2018–2020, project No. 53 (0367-2018-016).

References

1. Wegener, A.: The Origin of Continents and Oceans. Dover, New York (1966)
2. Replumaz, A., Capitanio, F.A., Guillot, S., Negredo, A.M., Villasenor, A.: The coupling of Indian subduction and Asian continental tectonics. Gondwana Res. **26**, 608–626 (2014). https://doi.org/10.1016/j.gr.2014.04.003
3. Lobkovsky, L.I.: Deformable plate tectonics and regional geodynamic model of the Arctic region and Northeastern Asia. Russ. Geol. Geophys. **57**, 371–386 (2016). https://doi.org/10.1016/j.rgg.2016.03.002
4. Likhanov, I.I., Regnier, J.-L., Santosh, M.: Blueschist facies fault tectonites from the western margin of the Siberian Craton: implications for subduction and exhumation associated with early stages of the Paleo-Asian Ocean. Lithos **304–307**, 468–488 (2018). https://doi.org/10.1016/j.lithos.2018.02.021

5. Cherepanova, Y., Artemieva, I.M., Thybo, H., Chemia, Z.: Crustal structure of the Siberian craton and the West Siberian basin: an appraisal of existing seismic data. Tectonophysics **609**, 154–183 (2013). https://doi.org/10.1016/j.tecto.2013.05.004
6. Domeier, M.: Early Paleozoic tectonics of Asia: towards a full-plate model. Geosci. Front. **9**, 789–862 (2018). https://doi.org/10.1016/j.gsf.2017.11.012
7. Vernikovsky, V.A., Metelkin, D.V., Vernikovskaya, A.E., Matushkin, N.Y., Kazansky, A.Y., Kadilnikov, P.I., Romanova, I.V., Wingate, M.T.D., Larionov, A.N., Rodionov, N.V.: Neoproterozoic tectonic structure of the Yenisei Ridge and formation of the western margin of the Siberian craton based on new geological, paleomagnetic, and geochronological data. Russ. Geol. Geophys. **52**, 24–39 (2016). https://doi.org/10.1016/j.rgg.2010.12.003
8. Müller, R.D., Qin, X., Sandwell, D.T., Dutkiewicz, A., Williams, S.E., Flament, N., Maus, S., Seton, M.: The GPlates portal: cloud-based interactive 3D visualization of global geophysical and geological data in a web browser. PLoS ONE **11**(3), 1–17 (2016). https://doi.org/10.1371/journal.pone.015088
9. Peryshkin, A.Y., Makarov, P.V., Eremin, M.O.: Numerical simulation of tectonic plates motion and seismic process in Central Asia. AIP Conf. Proc. **1623**, 487–490 (2014). https://doi.org/10.1063/1.4898988
10. Makarov, P.V., Peryshkin, A.Y.: Mathematical model and numerical simulation of slow deformation in the earth's crust structural elements. AIP Conf. Proc. **1783**, 020146 (2016). https://doi.org/10.1063/1.4966439
11. Seminskii, K.Z.: Hierarchy in the zone-block lithospheric structure of Central and Eastern Asia. Russ. Geol. Geophys. **49**, 771–779 (2008). https://doi.org/10.1016/j.rgg.2007.11.017
12. Goetze, C., Events, B.: Stress and temperature in bending lithosphere as constrained by experimental rock mechanics. Geophys. J. R. Astr. Soc. **59**, 463–478 (1979). https://doi.org/10.1111/j.1365-246X.1979.tb02567.x
13. Burov, E.B.: Rheology and strength of the lithosphere. Mar. Petrol Geol. **28**, 1402–1443 (2011). https://doi.org/10.1016/j.marpetgeo.2011.05.008
14. Stefanov, Y.P.: Some nonlinear rock behavior effects. Phys. Mesomech. **21**(4), 234–241 (2018). https://doi.org/10.1134/S1029959918030074
15. Smolin, I.Y., Makarov, P.V., Kulkov, A.S., Eremin, M.O., Bakeev, R.A.: Blow-up modes in fracture of rock samples and earth's crust elements. Phys. Mesomech. **21**(4), 297–304 (2018). https://doi.org/10.1134/S1029959918040033
16. Kozlovsky, Y.A.: The Superdeep Well of the Kola Peninsula. Springer, Berlin (1987)
17. Nikolaevskiy, V.N.: Geomechanics and Fluidodynamics with Applications to Reservoir Engineering. Kluwer, Dordrecht (1996)
18. Wilkins, M.L.: Computer Simulation of Dynamic Phenomena. Springer, Berlin (1999)

Formalized Forecast of the Gutenberg-Richter Law Parameters by Geodynamic and Seismotectonic Data

Eugeny Bugaev and Svetlana Kishkina

Abstract

Earthquake recurrence intervals have been compared with their estimated forecasting limits. The estimation was made taking into account the main fractal dimensions of the site, deformation conditions and destruction nature. The selected model demonstrated that the nonlinear recurrence intervals are determined by geological and geomechanical factors. It is proved that the estimation of forecasting recurrence interval limits can be possible on the basis of geodynamic data and limit seismotectonic relations that reflect the dependence of the maximum magnitude on the earthquake focus dimensions and destruction nature. The estimations are based on the example of the Calaveras fault area (California, USA), where it is possible to distinguish between the segments characterized by different creep rates. The analysis of the obtained results shows that the earthquake recurrence graph parameters of the investigated area significantly depend on its typical geological and geotechnical factors as area maximum structure size, similarity coefficient, conditions and deformation rate, destruction nature.

Keywords

Seismotectonic · Recurrence graph · Deformation · Fractal dimension

E. Bugaev
Scientific and Engineering Center for Nuclear and Radiation Safety,
Malaya Krasnoselskaya Street, 2/8, bld. 5, 107140 Moscow, Russia
e-mail: bugaev@secnrs.ru

S. Kishkina (✉)
Sadovsky Institute of Geospheres Dynamics RAS,
Leninsky prosp. 38, k.1, 119296 Moscow, Russia
e-mail: kishkinas@idg.chph.ras.ru

G. Kocharyan and A. Lyakhov (eds.), *Trigger Effects in Geosystems*,
Springer Proceedings in Earth and Environmental Sciences,
https://doi.org/10.1007/978-3-030-31970-0_2

1 Introduce

According Based on regional and local assessments of earthquake recurrence intervals, variations b from 0.3 to 2.5 [5] were established, as well as the level change of several magnitude recurrences during the transition from the quiescence to seismic activation period. The nature of the earthquake nonlinear recurrence intervals (hereinafter recurrence graphs) has not been clearly defined to date. The left and right bends of the recurrence graph can be explained by incomplete catalogs or computation methods [9]. The physical sources of these variations have been attributed to changes in strain condition [11, 17], loading rate [2, 18], and structural and compositional properties [17]. Low *b*-values are thought to be associated with high strain [12], low loading rate [13], low heterogeneity [10] and small fractal dimensions of the fault seismogenic surface [1, 8]. However, there are no specific accounting methods to analyze the effects of these multiple factors on the seismic regime parameters as slope and activity. Therefore, it is important to determine geological factors and their qualitative characteristics, which control the changes of earthquake recurrence graph.

The article proposes a method to assess the forecasting recurrence intervals based on the model that reflects discrete characteristics of the Earth crust and earthquake foci, as well as the natural dependence of the maximum magnitude on the focus size and the nature of its destruction. The model is characterized by the size of its maximum element corresponding to the length of the potential focus zone (hereinafter PFZ) related to the investigated area, and the similarity coefficient k_s equal to the square root of ten. This model allows taking into account the maximum period T_{max} related to accumulation of ultimate deformations in the maximum PFZ when the ultimate deformations reach the effective elasticε limit $\varepsilon_{eff} = 3.2 \cdot 10^{-5}$ for the Earth as a whole and the maximum PFZ is fractured. The flow rate of formation for various activated structures n is determined by the ratio of T_{max} to the number of rank structures n and up to the maximum element (n = 1) inclusive. Fractal curves are used to estimate the forecasting limits of the earthquake recurrence (hereinafter forecasting limits) taking into account the natural dependence of the maximum magnitude on the deformation conditions and the nature of the destruction [3].

The adopted method has been applied to geodynamic and seismic conditions of the Calaveras (California, USA) fault segment including the focus zone of the 1984 M 6.2 Morgan Hill earthquake (Fig. 1).

2 Seismic and Geodynamic Conditions and Model Parameters

Seismic conditions of the investigated area are listed in the Earthquake Catalog [15, 16], which is valid for M 3.5 and higher magnitude events for the observation period of 17 years, as well as for M 0.6 events for the observation period of about three years. The peculiarity of this catalog is that it includes data on the parameters

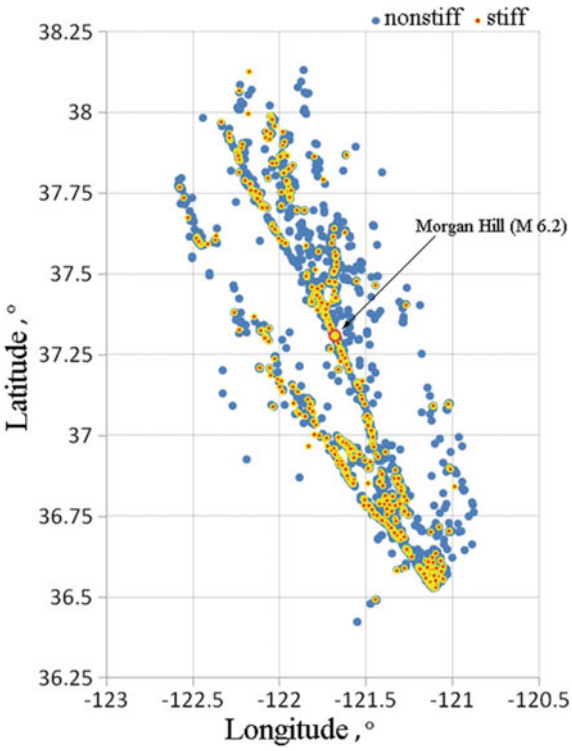

Fig. 1 Distribution of nonstiff (blue circles) and stiff (red circles) earthquake foci in the focal zone of the M 6.2 Morgan Hill earthquake (1984)

of the uncertainty ellipse related to the earthquake focus position. Taking into account high accuracy of determining foci to evaluate their deformation, the focus dimension was assumed as the maximum horizontal uncertainty ellipse axis [4]. The focus elastic limit ε is determined with account of the magnitude and focus size. The earthquake foci are divided into nonstiff $\varepsilon \leq \varepsilon_{\text{eff}}$ and stiff $\varepsilon_{\text{eff}} < \varepsilon \leq \varepsilon_{\text{br-pl}}$ taking into consideration the relation between ε and ε_{eff}, where ε is elastic limit, ε_{eff}—effective elastic limit equal to $\sim 3.2 \cdot 10^{-5}$. The brittle-plastic limit $\varepsilon_{\text{br-pl}}$ depends on the focus size and its impact (PFZ) and is determined as follows:

$$\log(\varepsilon_{br-pl}) = -0.5\log(L_0) + 0.5\log(L_{zone}) + \log \varepsilon_{eff} \tag{1}$$

where L_o—focus size, km; L_{zone}—focus effect zone length, km. The value of $\varepsilon_{\text{br-pl}}$ is a top physical elastic limit accumulated on the asperity. The relation (1) is obtained on the basis of empirical data on the dependence of the maximum deformation in the focus zone as well as on its size and on the ratio of the PFZ length to the maximum size of the PFZ's earthquake focus [6].

Nonstiff earthquakes are characterized by low seismic efficiency, whereas stiff earthquakes—by high seismic efficiency [6].

Calaveras fault is located in the zone of interaction between the Pacific plate and the North American platform constituting a right-hand shift. A specific feature of geodynamic conditions related to the Calaveras fault is its heterogeneity.

In terms of the investigated area, it is established that its North–Western segment is characterized by a low creep rate (less than 5 mm/year up to the locked sections), whereas for the South–Eastern segment, the creep rate reaches 25 mm/year and more [14]. Taking into account the area structure and geodynamic conditions, the main model characteristics have been adopted to allow a formalized assessment of the effective dimensions and the total number of constituent elements of the model rank n: size of the maximum model element equal to the maximum potential focus zone size L1 $\sim$ 320 (km); similarity coefficient k_s equal to the square root of ten; minimum ($Gmin \sim 1.8 \cdot 10^{-9}$ per year) and maximum ($Gmax \sim 4.1 \cdot 10^{-7}$ per year) deformation rate in the potential focus zone; *Gmin* characterizes the conditions of comprehensive deformation for the investigated area in general, and *Gmax* defines the conditions of uniaxial deformation for the fault central part.

The model type is determined by the deformation conditions, i.e. uniaxial deformation is relevant to the linear model with the fractal coefficient D equal to 1. Comprehensive deformation is relevant to the flat model where $D = 2$. According to the theoretical relationship between the fractal coefficient D and the slope b ($D/b = 2$), the effective value of the slope b is equal to 0.5 for uniaxial deformation, and 1—for comprehensive deformation, respectively. At the same time, for the strongest earthquakes, where the size of the foci tends to 1000 km, the slope b tends to 2 or more, which does not contradict to the data provided by Z. El-Isa and D.W. Eaton [5]. However, this above study [5] does not take into consideration the impact of deformation conditions and the nature of fracture related to b-value.

3 Diffusion of Earthquake Foci and Magnitude Recurrence Intervals

The analysis of earthquake foci diffusion in the impact zone of the Calaveras fault and the investigated area at different creep rates (Fig. 1) allowed to conclude that most stiff and nonstiff focis are into the principle zone of the Calaveras fault wich width is 0.6 km and less [7]; part of the nonstiff foci and single stiff events are manifested in the zone of the Calaveras fault dynamic impact with the width of about 20 km.

The Calaveras fault dynamic impact zone was also marked as the asymmetrical distribution of nonstiff foci: a smaller number of events are observed to the South–West of the locked section of the main rupture and to the North–East of the section with a high creep rate; while the North–East and South–West parts of the dynamic impact zone showed a larger number of events.

The conditions of uniaxial compression at the fault with a right-hand shift in its North–Western and South–Eastern regions of dynamic impact should indicate prevailing compression strains, while tensile strains should be present in the

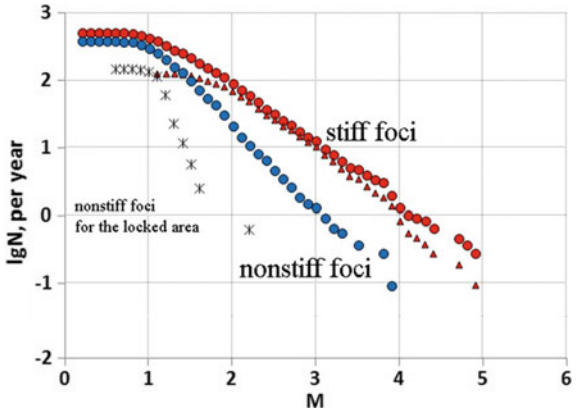

Fig. 2 Earthquake magnitude of both nonstiff and stiff earthquake recurrence graphs for Morgan Hill earthquake focal area. For comparison, graphs for regional (circles) and detailed (triangles) data and nonstiff foci for the locked area (asterisks) are shown

North–Eastern and South–Western. Compressive strains prevent the rearrangement of the structural plan while tensile strains contribute to it.

To analyze the creep effect on seismic regime parameters, recurrence intervals for the Morgan Hill earthquake focal area were estimated (Fig. 2). In Fig. 2, recurrence intervals of nonstiff foci are highlighted as blue and recurrence of stiff foci are highlighted as red. For comparison, graphs for regional and detailed data are shown.

The joint analysis of both nonstiff and stiff earthquake recurrence intervals allows to conclude the following: nonstiff foci events show a steeper slope compared to the stiff foci of the recurrence graph; slope b is more than in case with the creep events for the earthquakes in the locked part of the fault; nonstiff foci earthquakes associated with the creep section manifest clearly expressed nonlinearity of the recurrence graph; nonstiff foci earthquakes associated with the Morgan Hill earthquake zone also manifest nonlinearity and graph trend to bend downwards to the right; stiff foci earthquakes evidence less pronounced trend to nonlinearity for different observation conditions.

4 Comparison of Forecasting Limits with Recurrence Intervals

To identify the geological factors affecting the parameters of the recurrence, we compared them with the predicted limits (Fig. 3) estimated on the basis of the adopted model and geodynamic conditions of the investigated area. Zone "I" is the forecasting limits: line ($\varepsilon \leq 10^{-6}$) and line ($\varepsilon \leq \varepsilon_{eff}$) estimated for comprehensive

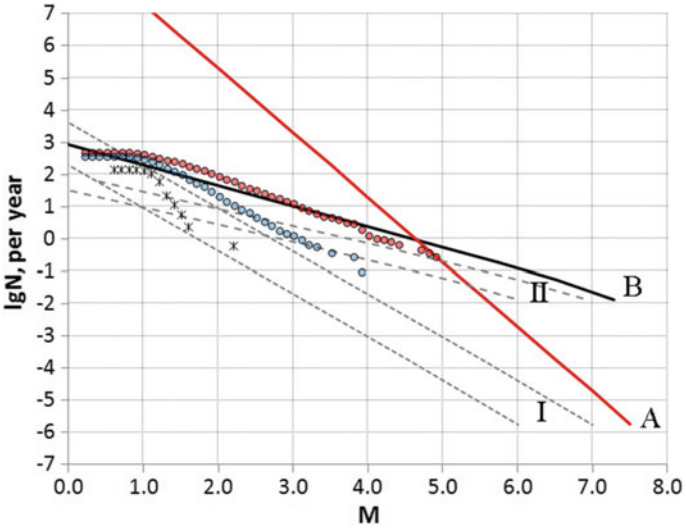

Fig. 3 A Comparison of the observed recurrent magnitude for nonstiff and stiff foci with the predicted limits estimated for different geodynamic conditions of deformation and destruction nature: zone "I"—forecasting limits of magnitude recurrent graphs for conditions of comprehensive deformation (up $\varepsilon \leq 10^{-6}$ to $\varepsilon \leq 3.2 \cdot 10^{-5}$); line "A"—most likely magnitudes of stiff foci ($\varepsilon > 3.2 \cdot 10^{-5}$); line "B"—forecasting limit for stiff foci under conditions of brittle-plastic destruction in case of uniaxial deformation ($\varepsilon > 3.2 \cdot 10^{-5}$); zone "II"—forecasting limits for weak foci in case of uniaxial deformation under conditions of brittle-plastic destruction ($\varepsilon \leq 10^{-6}$ and $\varepsilon > 3.2 \cdot 10^{-5}$ respectively)

deformation. Zone controls the recurrence graphs of nonstiff sources for the locked and for the creeping sections.

The recurrence diagrams of the Morgan Hill earthquake focal zone (blue circles in Fig. 3) slightly exceed one of the forecast limits (line 4 in Fig. 3), which may be due to a higher deformation rate or lower elastic limit in the focal zone than estimated. A higher deformation rate or a decrease in the elastic limit can be caused by the consolidation of the medium and an increase in its stiffness as a result of prolonged deformation and the preparation of a strong earthquake.

The recurrence graph position for stiff foci under different observation conditions is controlled by the top forecast limit of line "B" estimated for the conditions of uniaxial deformation and brittle-plastic fracture, and by bottom predicted limits for nonstiff sources (zone "II" from $\varepsilon \leq 10^{-6}$ to $\varepsilon \leq \varepsilon_{eff}$), estimated for the conditions of uniaxial deformation. It is likely that the recurrence graph bend on the right is physically stipulated by the impact of the brittle-plastic limit (1), the value of which decreases with the increase in the focus size.

5 Discussion

The analysis of the observed recurrence graphs for different geodynamic conditions and their comparison with the predicted limits of the recurrence graphs estimated for different deformation conditions and fracture nature allowed to establish main factors affecting the recurrence graph parameters.

Slope *b* is determined by deformation conditions and fracture nature: b = 1.33—at comprehensive deformation and brittle-plastic fracture; b = 0.64—at uniaxial deformation and brittle-plastic fracture; b = 1.07—at comprehensive deformation and brittle fracture; b = 0.55—at uniaxial deformation and brittle fracture.

Recurrence graph level (or seismic activity) is determined by the scale of the focus zone, elastic limit (or seismic impedance), and deformation rate. An increase in the process scale, a decrease in the elastic limit and medium consolidation, as well as an increase in the deformation rate during the activation of the seismic and geodynamic process can lead to a significant (by several orders of magnitude) increase in seismic activity. This was repeatedly observed in the last stage of catastrophic earthquake preparation; for example, the 1976 Tangshan earthquake in the North–Eastern area of the Chinese platform and the 2011 Tohoku earthquake in Japan.

Individual recurrence fragments are determined by the predicted limits estimated for different deformation conditions and fracture nature, so it is important to estimate the focus size and the amplitude of the adjustment movement in the focus.

Seismic process parameters are determined by a large number of geological, structural, geodynamic and geotechnical factors; lack of seismic statistical data complicates or makes it impossible to assess the seismic hazard on the basis of the probabilistic approach without taking into consideration a number of assumptions related to the Getenberg-Richter law linearity, constant value b = 1 (or close to it), and Mmax artificial limitation.

For low-activity and platform areas, it is recommended to perform seismic hazard assessment on the basis of geodynamic and seismotectonic data for different deformation conditions and fracture nature. The assessment validity of the forecasting limits is recommended to monitor by recurrent graph fragments estimated for different magnitude ranges with account of the limited but reliable historical and instrumental earthquake data, including paleoquakes and micro-earthquakes.

6 Conclusion

The analysis of the obtained results shows that the earthquake recurrence graph parameters of the investigated area significantly depend on its typical geological and geotechnical factors (area maximum structure size, similarity coefficient, conditions and deformation rate, destruction nature). The adopted method allows the following: assess seismic hazard on the basis of structural parameters of the investigated area, process scale, deformation conditions and destruction nature even